Photoinduced Fragmentation of Multilayer CH_3Br on Cu/Ru(001)

Tsachi Livneh*,† and Micha Asscher‡

Department of Physical Chemistry, Nuclear Research Center, Negev, P.O. Box 9001 Beer-Sheva 84190, Israel, and Department of Physical Chemistry and the Farkas Center for Light Induced Processes, The Hebrew University, Jerusalem 91904, Israel

Received: December 30, 2002; In Final Form: July 14, 2003

The broadband UV (230−420 nm) photoinduced chemistry of CH_3Br adsorbed on Cu(2ML)/Ru(001) in the coverage range of 1−50 ML was studied by monitoring the desorption products (Δp-TPD mode) in combination with post irradiation work function change measurements before and during surface heating ($\Delta\varphi$-TPD mode). $\Delta\varphi$ measurements enabled us to follow multilayer restructure and desorption of parent molecules and photochemical reaction products in the temperature range of 80−700 K. Methyl radicals accumulated on the surface are the precursor for the thermal formation of methane and ethylene at 450 K. Dehydrogenation of the methyl group is the rate-limiting step of the surface reaction resulting in the formation of these molecules. Based on work function change measurements, an estimate of the adsorbed methyl dipole moment is $\mu_0 =$ 0.48 D. Dissociative electron attachment (DEA) driven CH_3Br dissociation produced CH_3 and CH_2 fragments within the parent molecules multilayer matrix. At the multilayer coverage range, $\Delta\varphi$ increases by up to 1.1 eV after 10 min UV irradiation. Model calculations qualitatively describe the post irradiation work function changes induced by the embedded photofragments (mostly Br^- ions) inside the CH_3Br dielectric film. Comparison of the $\Delta\varphi$-TPD spectra on Cu(2ML)/Ru(001) to those on clean Ru(001) indicates that the nature of the molecule−surface interaction and the structure of the first few layers strongly influence the resulting photochemistry at layer thickness up to at least 20 ML.

1. Introduction

The photoinduced dissociation of methyl halides on well-defined surfaces has been extensively studied.[1] The motivation of these studies has been mostly to reveal the nature of the molecule-surface interactions under the influence of UV irradiation. The cross sections of the various processes were found to depend on the excitation wavelength,[2,3] adsorbate−surface distance and the dielectric properties of a spacer between them,[4] and predeposition of adsorbates[5]

Adsorbate photodissociation (at the 1−2 monolayers (ML) coverage) on metal surfaces is most likely to occur via dissociative electron attachment (DEA) mechanism:[1] $CH_3X_{(ad)} + h\nu \rightarrow CH_3X^{-}{}_{(ad)} \rightarrow CH_{3\,(gas/ad)} + X^{-}{}_{(ad)}$ (X = Cl, Br, I), in which a photoexcited substrate electron transfers to a surface stabilized anionic state of adsorbed CH_3X that promptly dissociates to give methyl radical and halide anion.

Photoexcited substrate electrons are generated with a broad energy distribution. A fraction of these primary or secondary electrons can attach to adsorbates molecular (affinity) levels that may reside under the vacuum level because of image dipole attraction with the metal substrate. As directly measured by Sanche and co-workers, electrons at kinetic energy of about 0.5 eV are sufficient to attach and cause DEA of methyl halides.[6]

Upon the formation of molecular multilayers, the direct dissociation route ($CH_3X_{(ad)} + h\nu \rightarrow CH_{3(gas/ad)} + X_{(gas/ad)}$) becomes increasingly dominant,[2,3] whereas the DEA channel is quenched, because of limited penetration into the multilayers of the ejected photoelectrons. The dependence of the photofragmentation yield on the number of deposited methyl halide layers was previously established for CH_3Cl/Pt(111)[7] by monitoring the dependence of the photolysis rates and photoelectron yields on the multilayer thickness, where mean free path was obtained for low energy (>1 eV) photoelectrons.

TOF (time-of-flight) measurements of photoproducts in the system CH_3Cl/Ni(111)[2] at excitation wavelengths of 193 and 248 nm were conducted. The CH_3Cl dissociation threshold energy and the high-energy peak of ejected methyl radicals were attributed to the direct dissociation channel, which is observed only at 193 nm. Although direct channel was observed at all coverages above 1−2 ML, the multilayer thickness necessary to totally quench the DEA process were ∼10 and ∼20 ML for excitation wavelengths of 248 and 193 nm, respectively. One may conclude that low energy photoelectrons generated from the “purely DEA” 248 nm photons could not reach the top layers at thickness that exceeds ∼10 ML, which nicely correlates with the measured penetration depth for low energy photoelectrons.[7]

A question arises how dominant is the “cage effect” in quenching the photodissociation within the molecular multilayers for the direct dissociation and the DEA channels. Previous studies have indicated that in the case of the direct dissociation channel, e.g., in the case of CD_3I multilayers on TiO_2(110) surface, methyl fragments that were detected by TOF were originated from molecules laying very close to the adlayer-vacuum interface. It was therefore concluded that the cage effect is significant and may be dominant within the adlayer.[8] Similar effects were observed in the case of photodissociation of CH_3I within rare gas matrixes.[9] However, this is not necessarily the case in the DEA channel. According to Marsh et al.,[2] even when electrons cannot reach the topmost layers, DEA may occur in

* To whom correspondence should be addressed. E-mail: tsaliv@netvision.net.il.
† Nuclear Research Center.
‡ The Hebrew University.

10.1021/jp027857y CCC: $25.00 © 2003 American Chemical Society
Published on Web 09/19/2003

the lower layers. This was demonstrated by monitoring the total cross section for parent molecules removal (CH_3Cl/Ni(111)) per incident photon[2].

The thermal chemistry of methyl and methylene halides on copper surfaces was previously studied.[10-14] The focus of these studies has been mainly kinetics and the mechanism of methyl and methylene dissociation and recombination and the effect of the copper surface structure. Surface reactions of C1 fragments were studied in various different systems such as CH_3I/Cu(110)[10] and CH_3I/Cu(111)[11,12] and CH_2I_2/Cu(110)[10,13] and CH_2I_2/Cu(100)[14].

Unlike the case of CH_3I, CH_3Br does not thermally dissociate on Cu(111),[15] and only minor dissociation products are detected at defects on the Cu(10 ML)/Ru(001) surface.[16] To initiate C1 surface reactions, the C−Br bond had to be cleaved by means of UV irradiation.[15-17] Br coverage was shown to play a significant role in the photochemical scheme by reducing the overall DEA cross section.[17]

Despite the extensive research of the photochemistry of methyl halides, very few studies explored the processes inside the multilayer. The chemistry of photogenerated fragments within the multilayer and irradiation induced multilayer rearrangements prior to and during surface annealing are practically unknown. The focus of this study is to examine the effect of broadband UV irradiation (230−420 nm) on the photo and thermal processes within CH_3Br multilayers deposited on Cu(2ML)/Ru(001) relative to the monolayer. An electrostatic model we present explains well the experimental data on the basis of photogenerated charges that are distributed within the molecular dielectric matrix, with the photoelectrons penetration depth as a parameter.

2. Experimental Section

The experiments described here were performed in an ultrahigh vacuum (UHV) chamber with a base pressure of 3×10^{-10} Torr obtained by turbomolecular pump (240 L/s). A sputter gun (Ar^+ ions at 600V and sample current of 8mμA) was employed to clean the Ru(001) surface and a quadrupole mass spectrometer (QMS-VG MASSTORR DX) was used to obtain Δp-TPD spectra. The QMS was surrounded by Pyrex shroud with 5 mm diameter aperture to minimize detection of desorbing species from surfaces other than the sample. A Kelvin probe (Besocke type S) was employed to monitor work function change ($\Delta\varphi$) as a function of crystal temperature using the same computer controlled routine. The heating rate was 2 K/s throughout this study.

The Ru(001) sample (a square piece, 8 × 8 mm, 1.5 mm thick) was cut from a single-crystal rod to within ±1° of the (001) crystallographic orientation and then polished by standard procedure. Sample cleaning procedure in UHV was described elsewhere.[18,19] LEED from the clean and annealed surface showed very sharp hexagonal pattern. The sample was attached to a liquid nitrogen reservoir via copper feedthroughs directly welded to the bottom of the dewar. AC resistive heating of two 0.5 mm diameter tantalum wires, between which the sample is spot welded, was employed to control the sample temperature. W5%Re − W26%Re thermocouple wires spot welded to the edge of the ruthenium sample were used for sample temperature determination and control.

CH_3Br (99.5% pure) was further purified by a few freeze−pump−thaw cycles to eliminate any noncondensable residual gases. Exposure was done by filling the chamber through a leak valve to the desired pressure with the uncorrected ion gauge signal transmitted to a computer and converted to Langmuir units (1 L = 10^{-6} Torr s).

Copper was evaporated onto the Ru(001) sample from a resistively heated Ta wire wrapped by high purity Cu wire (99.999%). The Ta filament was covered by a Pyrex shroud with 5 mm diameter aperture. The Cu source was thoroughly degassed prior to deposition and was controlled by monitoring the voltage drop across the Ta wire at constant current. The pressure rise during copper evaporation was routinely $1-2 \times 10^{-10}$ Torr. The sample was held during evaporation at 640 K in order to avoid CO adsorption and to produce well annealed surface, thus avoiding three-dimensional clustering of copper on the Ru(001) surface.

The copper coverage on the Ru(001) surface was kept constant at 2 ML throughout this work. At this copper coverage, the reactivity of the surface toward CH_3Br thermal decomposition has diminished relative to the clean ruthenium. The remaining minor reactivity is related to defects in the copper layers. The copper coverage was determined by (Δp-TPD)[20] at a heating rate of 9 K/s. The first layer desorption peak (with a maximum at 1235 K, at the completion of a monolayer) has a shape characteristic of zero order desorption kinetics, often taken as an indication for two-dimensional (2D) island formation within the adsorbed layer. Upon the full occupation of the second copper layer the maximum desorption peak is at 1150 K.

The irradiation source was UV enhanced 450 W Xe lamp manufactured by Oriel. IR irradiation was eliminated by means of a water filter. The light was focused at the surface by a series of quartz lenses covering the entire sample homogeneously. An Oriel 7−54 filter transmits the spectral range between 230 and 420 nm. This range avoids direct photodissociation of the adsorbed CH_3Br molecules. The photon flux of the lamp during UV illumination at the central wavelength (350 nm) was $\sim 3 \times 10^{16}$ photons/cm^2 s.

3. Results

The thermal chemistry of CH_3Br on Ru(001)[18] and over Cu(2ML)/Ru(001)[19] in the submonolayer and multilayer range was discussed elsewhere in detail. Briefly, the saturation coverage of the CH_3Br relative to the number of ruthenium atoms was determined to be 0.22 ± 0.02 for both surfaces[18] with the monolayer coverage (1 ML) consisting of $3.6 \pm 0.3 \times 10^{14}$ and $4.0 \pm 0.3 \times 10^{14}$ molecules/cm^2, respectively. The density of the crystalline CH_3Br in the (001) plane is 6.96×10^{14} molecules/cm^2, as obtained from X-ray studies.[21] Thus, it was concluded that upon completion of the first layer the density reaches 52 ± 5% and 58 ± 5%, respectively, of it's value in the bulk. We note that our interpretation of a monolayer is different from other studies[2-4,7] for which the definition of 1ML is correlated with a definition of a bilayer (2ML) in the present study.[18,19]

3.1. Photochemistry of 1 ML CH_3Br on the Cu(2ML)/Ru(001) Surface. *3.1.1. Δp-TPD.* Δp-TPD spectra are shown in Figure 1 of 1.1 ML CH_3Br (m/e = 94) and CH_4 (m/e = 16) from Cu(2ML)/Ru(001) following exposure to UV light (full spectral range, 230−420 nm) from a Xe lamp of up to 96 min of irradiation time. Without irradiation, only minor CH_4 desorption is observed, associated with parent molecules dissociation at defects on the copper layer that is subsequently followed by bimolecular reaction with adsorbed hydrogen to form methane. Cleavage of the C−Br bond is the result of the UV irradiation, producing "hot" CH_3 radicals. These radicals are either ejected to the gas phase or accumulated on the surface

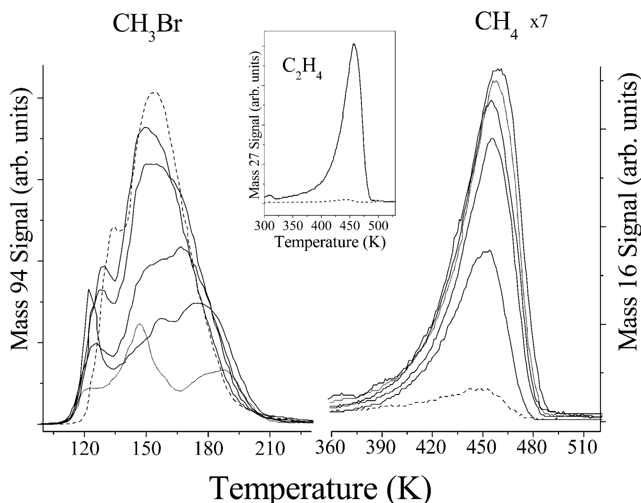

Figure 1. Δp-TPD spectra of 1.1 ML CH_3Br (m/e = 94) and CH_4 (m/e = 16) on Cu(2 ML)/Ru(001) following 0, 3, 6, 12, 24, and 96 min exposure to a UV Xe lamp at its full spectral range. The spectra for 0 and 96 min are denoted with dashed and dotted lines, respectively. In the inset: The C_2H_4 (m/e = 27) Δp-TPD after 12 min irradiation (solid line) and prior to irradiation (dashed line).

and disproportionate around 450 K to CH_4 and C_2H_4.[10,11] Finally, one cannot rule out the possibility of further photochemical dissociation of the adsorbed CH_3 radicals: Their first absorption band in the gas phase is around 216 nm[22] and the threshold of the adsorbed radicals that dissociate through the DEA mechanism is expected at a higher wavelengths, probably within our excitation range ($\lambda > 230$ nm). However, we expect this channel to be minor because our photon flux at these wavelengths is very low ($<10^{15}$ photons/cm^2 s).

As shown in the inset of Figure 1, the C_2H_4 signal clearly overlaps that of CH_4. A ratio of 3:1 was found between the integrated areas under the CH_4 TPD peak and that of C_2H_4. This ratio is higher than the expected 2:1 ratio based on the detailed mechanism for the methyl radicals disproportionation that was suggested by Bent and co-workers.[10,11] Such a discrepancy that was also found in other studies[11,16] may originate from complete methyl group dehydrogenation followed by carbon dissolution into the bulk.[11] It is interesting to note that the methane/ethylene ratio decreases in the multilayer coverage range toward the 2:1 ratio (see below), which may indicate that the channel of complete methyl dehydrogenation is becoming less favorable in the presence of accumulated bromine.

Although the integrated desorption peak of the parent molecule continuously decreases, the CH_4 and consequently C_2H_4 peaks increase only for irradiation times below 20 min and then are kept at constant surface coverage following longer irradiation times. The extent of CH_3Br dissociation (N_d) and the resulting CH_3 coverage are shown for various irradiation times, see Figure 2. After 24 min, the density of the photogenerated methyl radicals (extracted from the sum of the (calibrated) integrated TPD areas of CH_4 and C_2H_4) has saturated around CH_3/Cu(2ML)/Ru(001) = 0.04 ML. In light of a related study, where coadsorbed iodine atoms were found to decrease significantly (by a factor of 3) the saturation coverage of methyl radicals on Cu (111),[23] we conclude that the saturation density of the methyl radicals is influenced by the coverage of coadsorbed Br atoms on the Cu(2ML)/Ru(001) surface. Above a maximum coverage of the photochemicaly produced Br atoms, the methyl radicals are apparently ejected to the gas phase.

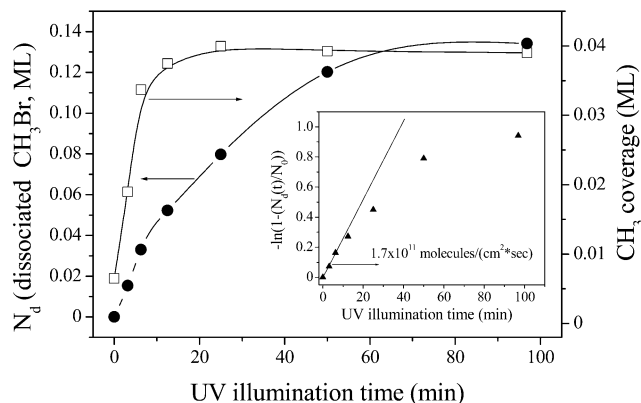

Figure 2. Extent of CH_3Br dissociation (N_d) and the resulting CH_3 coverage determined from Δp-TPD for different irradiation times. In the inset: $-\ln([CH_3Br](t)/[CH_3Br](0))$ vs UV illumination time is displayed.

Quantitative analysis indicates that after 96 min of irradiation 65% of the methyl radicals were ejected to the gas phase.

The photodissociation rate of methyl halides is expected to follow first-order kinetics in methyl halides concentration; therefore, it can be expressed

$$-\ln([CH_3Br](t)/[CH_3Br](0)) = kt \quad (1)$$

with

$$k = \sum_{\lambda} f(\lambda)\sigma(\lambda) \quad (2)$$

$f(\lambda)$ is the wavelength-dependent photon flux (photons/cm^2 s), $\sigma(\lambda)$ is the wavelength-dependent cross section for DEA (cm^2/photon), and t is the time of illumination. If the dissociation cross-section dependence on the surface coverage is negligible, $-\ln([CH_3Br](t)/[CH_3Br](0))$ is expected to vary linearly with the time of irradiation. In the inset of Figure 2, we note that initially, at short irradiation times, the photodissociation rate was $\sim 4 \times 10^{-4}$ ML/cm^2 s. Beyond 10 min deviation from linearity is observed, suggesting a decrease in the dissociation cross-section with time.

The origin of this saturation like behavior may be due to the following: (i) The increase in the surface work function due to the disappearance of methyl bromide and to the deposition of bromine atoms, see the discussion below. This increase may have shifted the affinity level of methyl bromide relative to the energy spectrum of the photoelectrons to a less favorable position in terms of electron attachment probability. (ii) Br (as an acceptor) and CH_3Br (as a donor) have opposite dipoles on the surface.[18,19,24] The consistent shift to higher temperatures of the CH_3Br Δp-TPD (Figure 1) and $\Delta\varphi$-TPD (see discussion below) as exposure to UV light increases suggests that attractive interactions between the coadsorbates (Br atoms and CH_3Br molecules) dominate. Consequently, stabilization of the ground electronic state may lead to more efficient quenching of the exited state and therefore the dissociation cross-section should further decrease.

3.1.2. $\Delta\varphi$-TPD. In Figure 3a, post irradiation $\Delta\varphi$-TPD spectra are shown of 1.1 ML CH_3Br/Cu(2ML)/Ru(001) following the indicated exposure times to the UV light. In the absence of irradiation, the work function is practically constant above 210 K, indicating no significant CH_3Br dissociation. Upon increasing the time of exposure, a peak around 450 K builds up. This peak coincides with the detected desorption of CH_4 and C_2H_4, as revealed in Figure 1. In Figure 3b, the derivative of the work

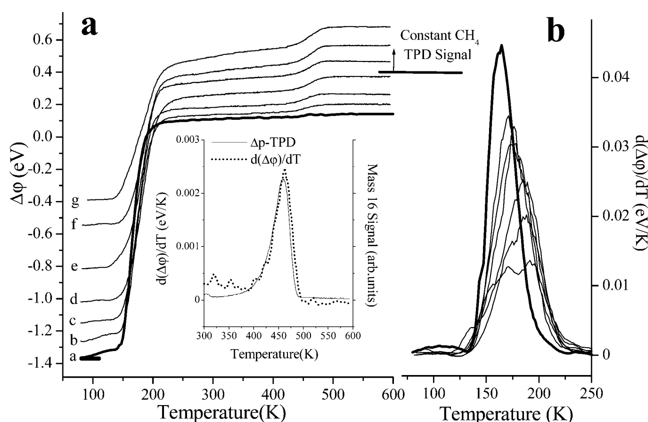

Figure 3. Post irradiation $\Delta\varphi$-TPD (a) $d(\Delta\varphi)/dT$ (b) spectra of 1.1 ML CH_3Br/Cu(2ML)/Ru(001) after exposure times of 0, 3, 6, 12, 24, 48, and 96 min (a−g, respectively) to the Xe UV full lamp. In the inset: A comparison of the Δp-TPD (solid line) and the $d(\Delta\varphi)/dT$ (dotted line) spectra around 450 K, indicating the very good overlap between the two.

function with respect to temperature $d(\Delta\varphi)/dT$ is presented. It is evident that, as bromine atoms accumulate on the surface, a shift to higher temperatures is observed in the derivative spectra. This reflects the stabilization of the methyl bromide molecules due to the presence of the bromine atoms, as a result of attraction between opposite dipoles (bromine= +0.8 eV/0.33 ML[24] and CH_3Br = −1.4 eV/0.22 ML[18]).

A comparison of the Δp-TPD and the $d(\Delta\varphi)/dT$ spectra around 450 K is shown in the inset of Figure 3a, indicating a very good overlap between the two. This is not surprising, considering that the desorption is rate limited by the methyl dehydrogenation $CH_3(a) \rightarrow CH_2(a) + H(a)$.[10] The reactions of methylene insertion and methyl hydrogenation were found to be considerably faster than the methyl dissociation on Cu(110).[10] Both the removal of CH_3 that is indirectly measured by work function change and CH_4 and C_2H_4 desorption are rate limited by the same step. Furthermore, the overlap between the two measurements suggest that, if methylene fragments simultaneously decompose in that temperature range as well, it must take place without affecting considerably the measured work function change.

The work function of the system increases by 0.12 eV upon removal of the methyl species from Cu(2ML)/Ru(001). Based on the integrated area under the corresponding methane Δp-TPD peak, the photochemically generated methyl coverage reached CH_3/Cu = 0.04 ML (0.18 of an initial 1 ML methyl bromide). Simple calculation based on the Helmholtz equation: $\Delta\varphi = 4\pi e N\mu_0$, where N is the surface methyl density, μ_0 is the isolated methyl dipole moment, e is the unit charge, provides an estimate of the isolated adsorbed methyl dipole moment of $\mu_0 = 0.48$ D (1 D = 3.34×10^{-30} C m). The justification to use this simplified model stems from the low coverage and insignificant dipole−dipole interaction between the methyl adsorbates.

As in the Δp-TPD case, a saturation value is reached also in the work function increase around 450 K after 12 min irradiation time. This observation suggests that at longer exposures to the UV light additional methyl radicals that are generated by the CH_3Br photodissociation, are ejected to the gas phase during the irradiation. However, further dissociation of CH_3Br following exposure to the UV light beyond 12 min (resulting in additional Br deposition on the surface) is evident from the increase in $\Delta\varphi$ at the completion of the $\Delta\varphi$-TPD run around 600 K. This result is consistent also with the monotonic decrease in the Δp-TPD signal of CH_3Br, as shown in Figure 1 at longer exposure times.

3.2. Photochemistry of Multilayers of CH_3Br on the Cu(2ML)/Ru(001) Surface. *3.2.1. Δp-TPD.* Δp-TPD spectra of CH_4 (m/e = 16) and C_2H_4 (m/e = 27) after 10 min UV irradiation of a Cu(2ML)/Ru(001) surface pre-deposited with 1−50 ML of CH_3Br are shown in Figure 4, parts a and b, respectively. The irradiation source is the same as in section 3.1; therefore, the direct dissociation channel of CH_3Br can be ignored while the surface temperature during irradiation was kept at 82 K

Around 1 ML coverage, ethylene and methane desorption signals practically overlap, having a single peak around 450 K, as discussed in section 3.1. As the coverage increases in the 3−22 ML range, the spectra change monotonically in the following manner:

1. A new desorption peak gradually emerges at 410 K on account of the 450 K desorption peak. Between 10 and 22 ML,

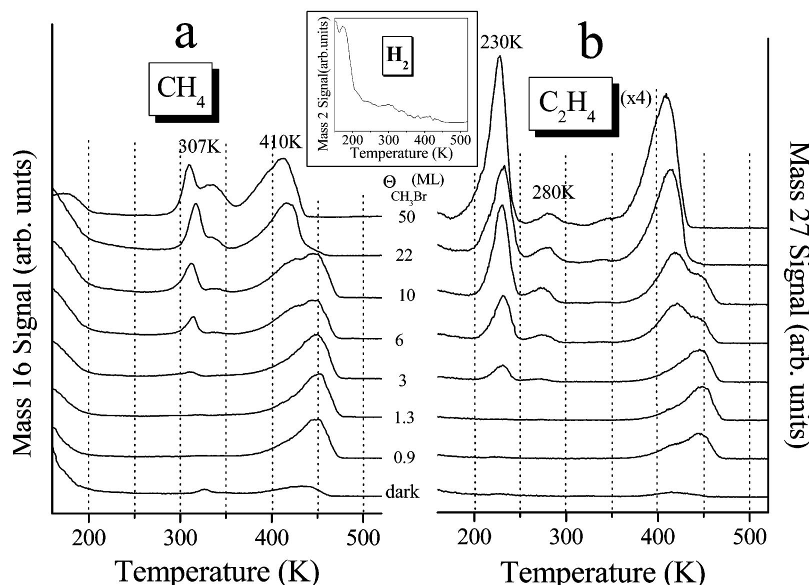

Figure 4. Δp-TPD spectra of CH_4 (m/e = 16) (a) and C_2H_4 (m/e = 27) (b) after 10 min UV irradiation time of a Cu(2 ML)/Ru(001) surface at 82K, predeposited with 1−50 ML of CH_3Br. The beam produced by the broadband irradiation source (Xe lamp) was filtered so that a 230−420 nm "window" was transmitted. In the inset: A typical Δp-TPD spectrum of H_2 (m/e = 2)

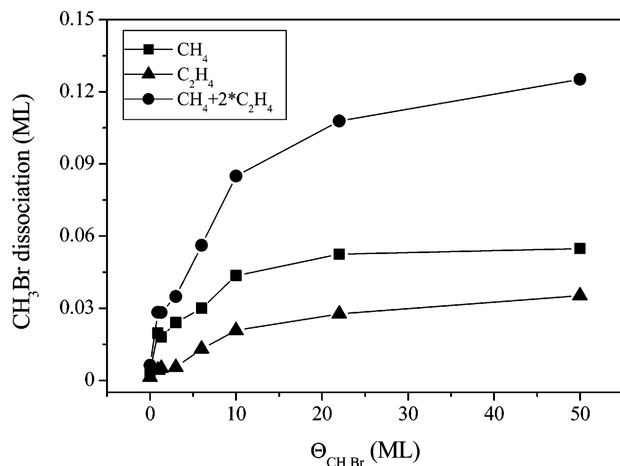

Figure 5. Dependence of the extent of CH_3Br dissociation on the layer thickness, as calculated by integrating the area under the Δp-TPD CH_4 and C_2H_4 peaks.

the peak around 450 K diminishes, whereas the peak at 410 K initially grows and then it saturates. The increased population in the 410 K peak on account of the 450 K peak is more pronounced for ethylene. 2. New peaks build up simultaneously around 307 and 330 K for CH_4 and around 230 and 280 K for C_2H_4.

In the inset of Figure 4, a typical Δp-TPD spectrum of H_2 ($m/e = 2$) is presented as well. Based on former studies which showed that hydrogen recombinative desorption from Cu(110) is expected around 340 K,[10] the absence of hydrogen desorption at this temperature range indicates that the hydrogen-methyl radical recombination to form methane is faster than hydrogen recombination and desorption, partially because of the high density of adsorbed methyl radicals.

The dependence of the extent of CH_3Br dissociation on the number of deposited layers, calculated by integrating the area under the CH_4 and C_2H_4 peaks in the Δp-TPD spectra, is shown in Figure 5. Based on the expected surface reaction pathways,[11] the $CH_4 + 2{*}C_2H_4$ signal is presented as well. The extent of dissociation steeply increases up to 10 ML, and at a reduced rate, it grows up to 22 ML coverage. Above 22 ML, no significant change in the Δp-TPD spectrum is observed.

3.2.2. $\Delta\varphi$-TPD. Because the overlap between the excitation spectrum (Xe lamp source) and the CH_3Br absorption spectrum was reduced to a minimmum (using a proper optical filter) the main photodissociaction channel left is a DEA surface mediated processes, upon which Br^- ions are produced within the CH_3Br matrix.[2,6,25] These ions generate electric field around them and are attracted to their image charge inside the bulk metal underneath. To caracterize the dissociation products embedded inside the multilayer structure after irradiation and to probe the multilayer restructure during the diffusion of the Br^- ions, a set of $\Delta\varphi$-TPD spectra were recorded under similar condition as for the Δp-TPD. These are shown in Figure 6. For comparison, the $\Delta\varphi$-TPD of 4 ML CH_3Br that have not been exposed to UV light is shown by dotted line.

The increase in the work function that resulted from photodissocoation of gradually thicker layers of CH_3Br following 10 min irradiation at 82 K is shown in the inset of Figure 6. An increase of the work function of up to 1.1 eV was measured (note that $\Delta\varphi$ of the 50 ML CH_3Br was -0.8 eV prior to irradiation because $\Delta\varphi$ upon adsorption at 82 K gradually increases after the completion of the second layer[19]). In addition, the signature of methyl radical dissociation and the desorption

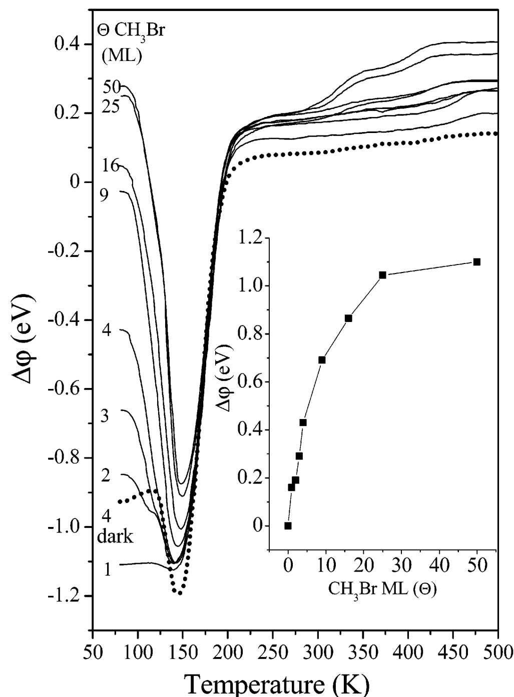

Figure 6. $\Delta\varphi$-TPD spectra after 10 min UV irradiation time of a Cu(2 ML)/Ru(001) surface predeposited with 1−50 ML of CH_3Br. For comparison, the $\Delta\varphi$-TPD of 4 ML CH_3Br that have not been exposed to UV light is shown by dotted line. In the inset: A summary of the increase in the work function resulted from photodissocoation of gradually thicker CH_3Br layers, following 10 min irradiation.

of its producs from the Cu(2ML)/Ru(001) surface is monitored at $T > 250$ K. The increase in $\Delta\varphi$ due to methane and ethylene production gradually shifts from 450 K down to 280 K upon increasing CH_3Br layer thickness up to ~25 ML. Above this coverage, no further change in the $\Delta\varphi$ profiles is observed, consistent with the Δp-TPD results of Figure 4.

Information on surface processes that occur at coverages and temperatures below the onset for molecular desorption can be obtained from $\Delta\varphi$-TPD spectra. In Figure 7a,b, we present the Δp-TPD (Figure 7a) and the $d(\Delta\varphi)/dT$ spectra (Figure 7b) of CH_3Br in the 80−150 K range. The temperature ranges for the desorption of the different layers of CH_3Br are indicated. Comparison of the desorption onset of condensed CH_3Br with the $d(\Delta\varphi)/dT$ spectra illustrates that a significant change in the work function is recorded during sample heating before any desorption takes place. This process is observed only after the system has been irradiated. No $\Delta\varphi$ change for the nonirradiated system could be detected prior to the multilayer desorption temperature (dashed line in Figure 7b). The peaks obtained at temperatures preceding desorption may arise from diffusion of DEA products to the surface and multilayer restructure. However, these processes need further investigation before we fully understand them.

Differential spectra $d(\Delta\varphi)/dT$ at temperatures where the dissociation products react and desorb as new product molecules are shown in Figure 7c. We note the shift of the desorption peaks to lower temperatures, similar to the corresponding Δp-TPD spectra shown in Figure 4. The overlap between $d(\Delta\varphi)/dT$ and Δp-TPD of methane is demonstrated for a layer of 22−25 ML in Figure 7c. The overlap between the two for the monolayer coverage range was attributed to the methyl dissociation ($CH_3 \rightarrow CH_2 + H$) being the rate-determining step, followed by a rapid process of recombinative desorption of methane due to reaction of adsorbed hydrogen atoms with

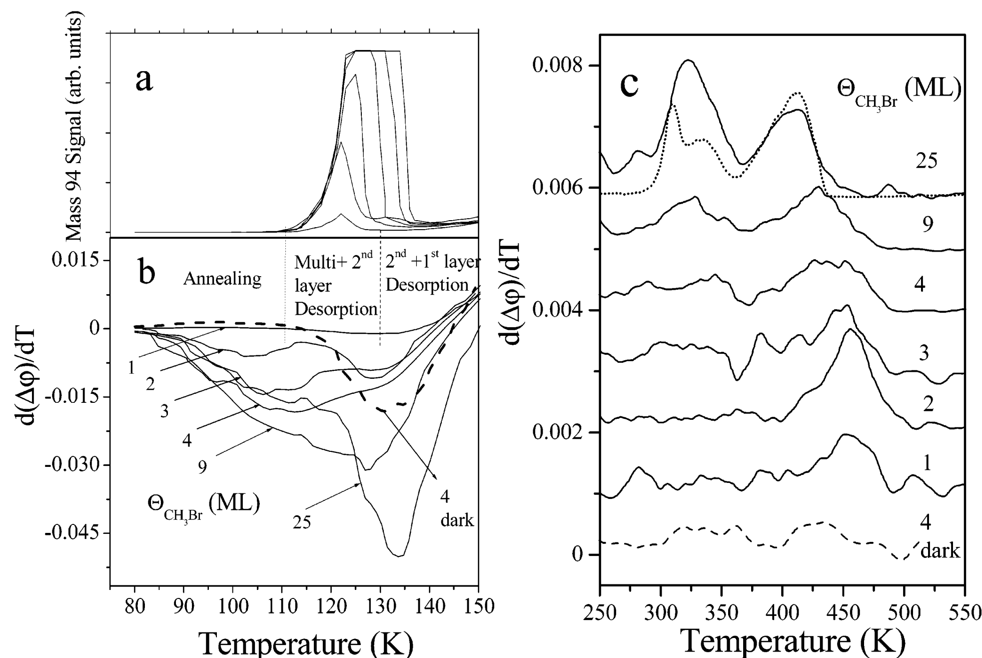

Figure 7. Δp-TPD (a) and the d($\Delta\varphi$)/dT spectra (b) of CH_3Br in the 80−150 K range. The temperature range for the desorption of the different CH_3Br layers is indicated. (c) d($\Delta\varphi$)/dT spectra at higher temperature range of 250−550 K, where methyl dehydrogenates, see text. Δp-TPD of methane for irradiated 22 ML and the (d($\Delta\varphi$)/dT) of 4 ML CH_3Br that have not been exposed to UV light are also shown for comparison.

adjacent methyl.[10] The presence of photo generated Br atoms as coadsorbates on the surface during this reaction suggests that despite a shift in the desorption temperature by 40 K, it did not change the overall kinetic scheme of the methyl dehydrogenation as a rate-limiting step. This is consistent with studies by Bent et al.,[23] where iodine poisoning was reported as a minor perturbation to the overall scheme of the methyl radical dissociation on Cu(111).

When multilayers undergo DEA, the density of photoproducts on the surface is expected to be significantly higher, as a result of accumulated DEA products from at least 20 ML. Nevertheless, the overall behavior at the 250−550 K temperature range seems very much the same as the monolayer coverage case. This except for the typical second-order kinetics shift to lower temperatures as coverage increases.

3.3. Multilayer CH_3Br on Ru(001) vs Cu(2ML)/Ru(001). The thermal chemistry and structure of multilayer methyl bromide on Ru(001)[18] and Cu(2ML)/Ru(001)[19] were previously reported. A question arises as to what is the influence of the under laying metallic substrate on the photochemistry within the multilayer: How the dissociation cross section inside the matrix may be sensitive to it and to what extent the matrix restructure can be affected by the substrate. Destabilization of the third layer and then a more stable fourth and thicker layers on the clean Ru(001) were discussed in terms of bulklike molecular crystalline structure formation.[18] It turns out that on the copper covered surface destabilization of the third layer is not observed. Based on work function change measurements taken during adsorption, we concluded that, unlike the clean Ru(001) surface, on the Cu(2ML)/Ru(001) surface, CH_3Br molecules do not form the molecular crystalline-like structure based on antiparallel arrangement. This may be related to the high density of defects on the Cu(2ML)/Ru(001) surface. Such defects will often lead to molecular adsorption in a wide distribution of tilt angles with respect to the surface normal, thus avoiding the necessary packing that results in the molecular crystal structure.

In Figure 8a, the $\Delta\varphi$-TPD spectra of CH_3Br(9ML)/Ru(001) at 82 K before and after irradiation are compared. Following 10 min irradiation, an increase of 1.5 eV in the work function is observed. However, upon annealing the surface to temperatures still below the parent molecule desorption onset at 110 K, the surface work function is practically recovered to the value in the absence of irradiation. It is evident that photodissociated fragments and multilayer restructure prior to desorption are responsible for a significant work function decrease of ~1 eV. In Figure 8b, (d$\Delta\varphi$/dT) spectra are compared for Ru(001) and Cu(2ML)/Ru(001). It is clear that $\Delta\varphi$ prior to multilayer desorption is more pronounced on Ru(001) than on the Cu(2ML)/Ru(001) surface. Furthermore, the work function change flips its sign from positive on the nonirradiated Ru(001) to negative change upon exposure to the UV light, as shown for 9 ML CH_3Br in Figure 8b. This can be attributed to the presence of Br^- union within the multilayer and the graduate process of charge-transfer back to the substrate upon annealing.

Three processes are expected to occur in the matrix:

(i) Multilayers restructure. (ii) Attraction of the Br^- ions by their image charge in the bulk metal that results in their migration toward the surface. (iii) Dissociation of caged negative ion complexes, $(CH_3Br)_n^-$, $n \geq 1$ that are created as a solvation-like process that stabilizes the ionic species.[6] Ethane (mass 30) and ethylene (mass 27, the choice of this mass was to avoid the large background at mass 28) TPD peaks are observed near 95 K. These molecules are absent from the TPD spectra in the case of the nonirradiated system. The peak near 95 K, shown in Figure 8c, practically coincides with the minimum of the d$\Delta\varphi$/dT spectrum, shown in Figure 8b. The methane peak (not shown) was also observed. These ethylene and ethane peaks probably originate from methyl recombination and methylene insertion of some of the CH_3 and CH_2 dissociation products that are free to diffuse, react, and desorb upon annealing the multilayer. The correlation between the dissociated fragment diffusion/reaction/desorption and a significant restructure in the multilayer reflects a "phase transition-like" behavior that allows

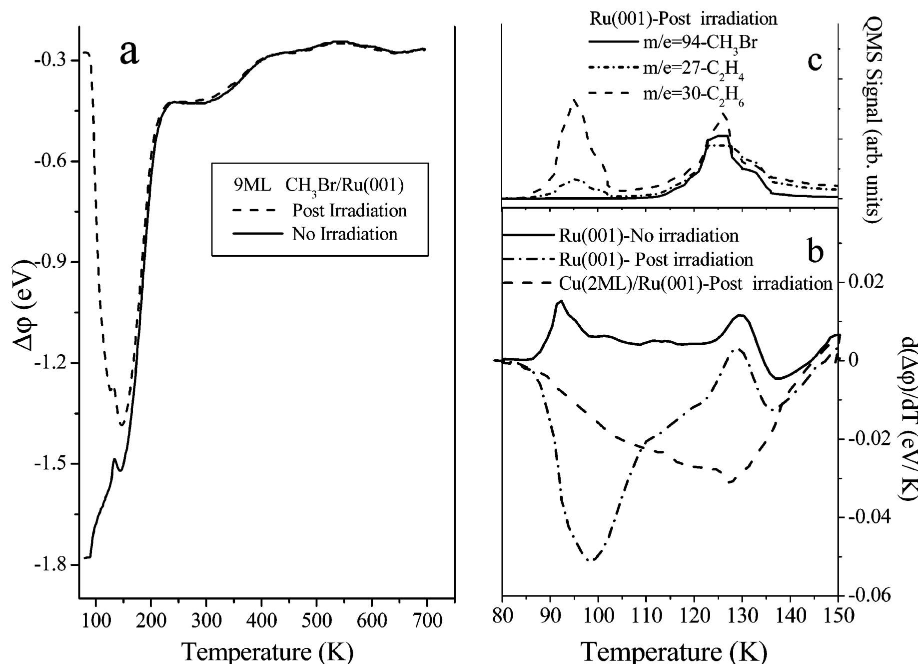

Figure 8. (a) $\Delta\varphi$-TPD spectra of CH_3Br(9 ML)/Ru(001) at 82 K before and after irradiation. (b) ($d\Delta\varphi/dT$) spectra of CH_3Br(9 ML)/Ru(001) before and after irradiation and CH_3Br(9 ML)/Cu(2 ML)/Ru(001) following irradiation. (c) Δp-TPD spectra of C_2H_4 (m/e = 27, dashed−dotted line), C_2H_6 (m/e = 30, dashed line), and CH_3Br (m/e = 94, solid line) after 10 min UV irradiation of a Ru(001) surface, predeposited by 9 ML of CH_3Br.

a vast reorganization in the multilayer. However, the fact that the $d\Delta\varphi/dT$ spectrum of the nonirradiated multilayer is peaked (having an opposite sign) in the same temperature range before the desorption onset of the parent molecules (see Figure 8b) indicates that this behavior is a unique property of the CH_3-Br−Ru(001) system. This behavior should be associated with the different packing of the first 4 layers (see refs 18 and 19 for elaborate discussions). Photochemically produced fragments seem to enhance this phenomenon.

Another interesting difference between the two substrates that is revealed by photochemistry is the different $\Delta\varphi$-TPD spectra obtained at temperatures above the CH_3Br desorption, $T > 210$ K. As demonstrated in Figure 8a, the $\Delta\varphi$-TPD profiles of the irradiated and nonirradiated multilayers are identical above 150 K in the case of clean Ru(001). This indicates that the photogenerated fragments do not modify the distribution of species that are formed and stabilized on the surface upon annealing at temperatures above 210 K. This is not the case for the Cu(2ML)/Ru(001) surface shown in Figures 4 and 6. It may be correlated with the lower reactivity of both adsorbed CH_3Br and CH_3 radical on this copper character-like surface.

4. Discussion

4.1 Multilayer Film Irradiated at 82 K. In the following, we present a simplified electrostatic model that attempts to address the experimental observations of work function increase of 1.1 eV upon UV irradiation of multilayer methyl bromide. For our system of CH_3Br on Cu(2ML)/Ru(001) at 82 K, three assumptions can be made based on earlier studies:[2,3,6,7]

(i) No significant direct photodissociation channel takes place. (ii) The maximum penetration depth of photoelectrons is ~20 ML. (iii) For simplicity, we take an average value of the DEA cross section to represent the fact that we neglect its layer thickness dependence.

Quantitatively, there are two different aspects of coverage that were identified in our Cu(2ML)/Ru(001) experiment: (i) The extent of dissociation measured by the integrated signal of CH_4 and C_2H_4 should reflect the production yield of Br atoms, based on negligible thermal dissociation. (ii) The work function change at 82 K that is due to photofragments contribution (mostly Br^- ions) that are captured within the CH_3Br matrix following UV irradiation.

Because bromide ions are expected to significantly affect the work function, we shall treat the ionic influence using a modified electrostatic model that was originally developed by Tsekouras et al.[26] for ions *on* hydrocarbon films.

A certain concentration of bromide ions are placed on top of a condensed CH_3Br layer deposited on a metal surface. This layer is expected to act as an insulating linear dielectric medium. Ions placed on top of it should create a voltage because of their charge and the capacitance of the film. This voltage creates a change in the work function φ of the metal+film assembly by an amount of

$$\Delta\varphi = \frac{-eQL}{A\epsilon\epsilon_0} = -eV_{\text{film}}$$

where Q is the charge deposited, A is the area, L is the film thickness, ϵ is the dielectric constant of the film, ϵ_0 is the vacuum permittivity, and e is the unit charge. If ϵ is constant throughout the film, diffusion of ions should lead to a change in the lateral distribution of the ions inside the film $\rho(x,y,z)$. As a thermally activated process, diffusion is accelerated by annealing of the molecular matrix. At 82 K, we assume that the ions are frozen at the coordinates where DEA took place. The time dependent distribution of vertical distances of ions from the surface inside the film can be followed by monitoring the change in the work function. Generally, the x and y dependence should be rather small for a macroscopically homogeneous film, which is sensitive only to the density average over x and y, to give $\rho(z)$. Integration by parts of the Poisson equation over the free charges in the presence of constant dielectric medium yields a simple expression for the change in the work function that

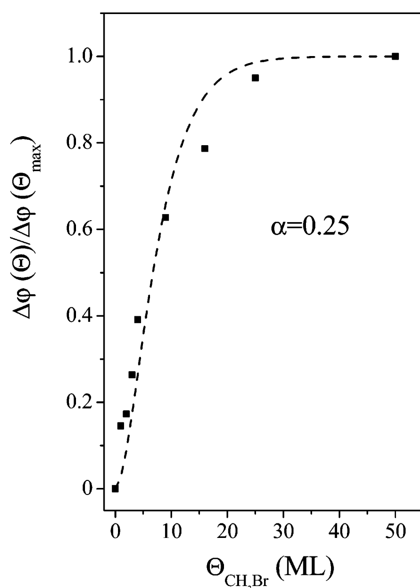

Figure 9. Normalized work function change $\Delta\varphi(\theta)/\Delta\varphi(\theta_{max})$, following 10 min irradiation time at 82 K as a function of methyl bromide layer thickness in ML. The dashed line is the calculated curve, see text.

results from the voltage across the film:[26]

$$\Delta\varphi(L) = -e(V(L) - V(0)) = -\frac{e}{\epsilon\epsilon_0}\int_0^L z\rho(z)\,\mathrm{d}z \quad (3)$$

Therefore, we can use this picture of a frozen distribution of ions inside a dielectric medium as a valid description of our system after irradiation at 82 K. It is necessary to define $\rho(z)$ more precisely as follows:

$$\rho(z) = \sum_{\lambda} F(\lambda)\, N_e(\lambda) e^{-\alpha\cdot z} k_{Br} \quad (4)$$

$F(\lambda)$ is the time integrated flux density of photons weighted by the wavelengths profile of the irradiation source. $N_e(\lambda)$ is the wavelength dependent probability of ejecting a low energy photoelectron. $\sum F(\lambda)N_e(\lambda)$ is therefore the time integrated flux density of photoelectrons that are ejected from the surface. The dependence of slow photoelectrons penetration on z is of exponential form where $1/\alpha$ is the penetration depth, assumed to be independent of their energy below 1 eV.[7] In order to estimate the number of ions produced at a certain infinitesimally small dz distance along the dielectric layer, we introduce k_{Br} as the number of ions (mostly Br^-) that are produced per photoelectron. We neglect the dependence of k_{Br} on z, which is an approximation that becomes more accurate as the ions are removed away from the surface−film interface, where image charges do not play a significant role.

In Figure 9, we demonstrate the correspondence between the calculated expression

$$\frac{\Delta\varphi(\Theta)}{\Delta\varphi(\Theta)_{max}} = \frac{\int_{\Theta}^{0} z\rho(z)\,\mathrm{d}z}{\int_{\Theta_{max}}^{0} z\rho(z)\,\mathrm{d}z}$$

to the experimental values of the work function change at 82 K after 10 min irradiation as they vary with the layer thickness. $\Delta\varphi(\Theta)$ is extracted from the data presented in Figure 6, normalized to $\Theta_{max} = 50$ ML, where no changes in $\Delta\varphi$ were further observed. Converting the fitted parameter α to the number of monolayers results in a penetration depth of 4 ML. The coverage dependence of the photo fragmentation was previously established for the CH_3Cl/Pt(111) system by measuring the photolysis rates and low energy (<1 eV) photoelectron yields as a function of thin layer thickness, and a penetration depth of 1.8 ML was reported,[7] which is similar to ours.[27] We may consider the quality of the fit in Figure 9 as supporting evidence for the claim that ions and electrons have long-range polarization effects on the neutral dielectric films they are embedded within and therefore justify the employment of the ion-dielectric formalism in order to describe embedded charges inside a multilayer.

The cage effect has often been considered to be the main reason for relatively small measured cross sections for photodissociation of molecules embedded in a matrix.[9] The cage created by the surrounding atoms or molecules introduces a barrier for dissociation that originates from the need of the photofragments to escape the cage walls. However, if a low energy photoelectron is ejected from the surface to be attached to a parent molecule within the multilayer, an externally assisted anionic bound state, $(CH_3Br)_n^-$, $n \geq 1$, may be formed.[6] Such a "solvation" process should stabilize the anion via polarization of the surrounding medium. A recent study has reported a DEA cross section of $\sim 1 \times 10^{-16}$ cm^2 for low energy electrons near and below 1 eV, for CH_3Cl molecules embedded inside a Kr solid matrix. This value is seven times higher than that of CH_3-Cl when deposited *on top* of a Kr solid surface.[6] The difference between the surface and bulk photoinduced processes was attributed to unique product stabilization in the bulk that overcomes the decrease in the cross section due to the cage effect. Similar cross sections were reported for CH_3Br molecules condensed on top of a Xe film as well as with a maximum DEA cross section for electrons at kinetic energy of 0.1 eV. These values are more than two orders of magnitudes higher than the equivalent DEA cross section in the gas phase.[25]

One may conclude that there is an interplay between stabilization effects and escape probability from a cage of the dissociated fragments that dictates the net probability for the DEA process of an embedded CH_3Br molecule. Voids in the amorphous solid that reduce the perfect cage structure may also reduce the cage effect in favor of enhancing DEA. Because our measurements are based on macroscopically averaging work function changes measured at 82 K, it is impossible for us to distinguish between the separate contributions of Br^- ions (DEA products) and stabilized $(CH_3Br)_n^-$ cluster ions.

4.2. Fragmentation within the Multilayer. A notable difference is observed between the photochemical formation rates of CH_4 and C_2H_4 at 1 ML coverage of CH_3Br on Cu-(2ML)/Ru(001) to the rates observed at a coverage of 22 ML on the same substrate. At the high coverage, the photoproducts may further react only after the annealing/desorption of the multilayer. A significant difference in the peak desorption temperatures of these two products is observed. The desorption peak shifts from 450 K at 1 ML to 410 K at 22 ML, following exposure to the UV irradiation. This shift is attributed to the higher density of photogenerated CH_3 radicals that were formed within the ~25 ML thick film and are accumulated on the surface upon annealing. Higher density of adsorbed methyl radicals leads to a faster and, therefore, lower temperature reaction. We believe that the second-order kinetics appearance of these products, suggest a disproportionation reaction to take place between two adjacent methyl groups:

$$2CH_3(a) \rightarrow CH_4(g) + CH_2(a)$$

The dominance of this second order reaction can be understood only at higher coverages. At the lower ones, methyl dehydrogenation is the rate-limiting step, as discussed before. Second-order kinetics explains in a trivial way the increasing yield and the shift of products appearance to lower temperatures.

Very low temperature for ethylene formation near 230 K, is observed as a result of the multilayer photochemistry. The C_2H_4 peak centered at 230 K is attributed to CH_2 radicals recombination: $2CH_2(a) \rightarrow C_2H_4(a)$ to form ethylene that desorbs immediately upon formation. Similar results were obtained on single-crystal Cu(100).[14] The CH_2 radicals may originate from further photodissociation or DEA of methyl radicals at 82 K inside the multilayer structure. Electron attachment to the CH_3 radical is known to stabilize it while removing its planarity. The existence of the methide (CH_3^-) ion was demonstrated and shown to have electron affinity of 0.08 ± 0.03 eV.[28]

After the C_2H_4 desorption peaked at 230 K, another C_2H_4 production channel is observed, its maximum rate is around 280 K, followed by a CH_4 desorption at 310 K. The 280 K C_2H_4 peak, that was detected also on Cu(100),[14] is thought to proceed via methylene insertion mechanism $CH_2(a) + CH_3(a) \rightarrow C_2H_4(a) + H(a)$.[10] The subsequent 310 K peak is due to CH_3 hydrogenation by the hydrogen atoms that are supplied from the above methylene insertion.[10] It is important to note that no H_2 is produced concurrent with CH_4 desorption, probably because CH_3 coverage is significantly higher than the H atoms coverage.

Around 450K desorption peaks due to CH_4 and C_2H_4, are observed to shift to lower temperatures with increasing multilayer coverage, as discussed above. The C_2H_4/CH_4 ratio increases by a factor of 2 as the CH_3Br initial coverage increased from 1 to 22 ML. The integrated C_2H_4 desorption signal at low temperatures (230 K) is higher than that of CH_4. It may be that both rate constants of CH_3 hydrogenation ($CH_3(a) + H(a) \rightarrow CH_4(g)$) and methylene insertion ($CH_2(a) + CH_3(a) \rightarrow C_2H_4(a) + H(a)$) are affected in a different way from the increase of the Br coverage and the rate of methylene insertion is amplified on account of methyl hydrogenation.

5. Conclusions

The broadband UV (230−420 nm) photoinduced chemistry of CH_3Br adsorbed on Cu(2ML)/Ru(001) in the 1−50 ML coverage range was studied by monitoring the desorption products (Δp-TPD mode) in combination with post irradiation work function change measurements before and during surface heating ($\Delta\varphi$−TPD mode). The later enabled us to follow changes in $\Delta\varphi$ that are due to multilayer restructure and desorption of the photoproducts in the 80−700 K temperature range.

Methyl bromide undergoes dissociative electron attachment (DEA) at the photoexcitation wavelengths used in this study.

At 1 ML CH_3Br, the initial coverage maximum density of the photo generated CH_3 radicals is equivalent to 0.04ML. Any additional DEA produced methyl radical is ejected to the gas phase. The adsorbed CH_3 radicals were found to disproportionate during surface heating around 450K to produce $C_2H_4 + CH_4$ in a 1:3 ratio. Simple calculation, which is based on work function change measurements, provides an estimate of the isolated adsorbed methyl dipole moment of $\mu_0 = 0.48$ D.

With increasing initial CH_3Br coverage from 1 to 22 ML the CH_4 and C_2H_4 peaks around 450 K are shifted to 410 K and the C_2H_4/CH_4 ratio increases by a factor of 2. Enhanced CH_2 production due to photochemistry within the multilayer is revealed by the lower temperatures (230 K) ethylene production and desorption.

DEA driven CH_3Br dissociation produced CH_3 and CH_2 fragments inside the multilayers. The maximum equivalent coverage of the trapped methyl radicals increases up to 0.06 ML at 22 ML initial parent molecules layer thickness.

At the multilayer coverage range, $\Delta\varphi$ increases up to 1.1 eV after 10 min irradiation. We present an electrostatic model that qualitatively explains the post irradiation work function increase induced by the embedded photofragments (mostly Br^- ions) inside the CH_3Br dielectric film. Using the formalism of the above model to fit the experimental data we obtain a penetration depth for low energy photoelectrons of 4 ML onto the molecular layer, in agreement[27] with prevously reported data for CH_3Cl/Pt(111).[7]

Comparing the $\Delta\varphi$-TPD spectra obtained for CH_3Br on Cu-(2ML)/Ru(001) to that on clean Ru(001) surfaces indicate that the nature of the molecule-surface interaction and structure of the first few layers significantly influences the photochemistry up to at least 20 ML.

References and Notes

(1) Zhou, X. L.; Zhu, X. Y.; White, J. M. *Surf. Sci. Rep.* **1991**, *13*, 73.
(2) Marsh, E. P.; Tabares, F. L.; Gilton, T. L.; Meier, W.; Schneider, M. R.; Cowin, J. P. *Phys. Rev. Lett.* **1988**, *61*, 2725.
(3) . Marsh, E. P.; Tabares, F. L.; Schneider, M. R.; Gilton, T. L.; Meier, W.; Cowin, J. P. *J. Chem. Phys.* **1990**, *92*, 2004.
(4) Gilton, T. L.; Dehnbostel, C. P.; Cowin, J. P. *J. Chem. Phys.* **1989**, *91*, 1937.
(5) Solymosi, F.; Kiss, J.; Révés, K. *J. Chem. Phys.* **1991**, *94*, 8510.
(6) Ayotte, P.; Gamache, J.; Bass, D.; Fabricant, I.; Sanche, L. *J. Chem. Phys.* **1997**, *106* (2), 749.
(7) Jo, S. K.; Zhu, X. Y.; Lennon, D.; White, J. M. *Surf. Sci.* **1991**, *241*, 231.
(8) Holbert, V. P.; Garrett, S. J.; Stair, P. C.; Weitz, E. *Surf. Sci.* **1996**, *346*, 189.
(9) Bondybey, V. E.; Burns, L. *Adv. Chem. Phys.* **1980**, *41*, 269.
(10) Chiang, C.-M.; Wentzlaff, T. H.; Bent, B. E. *J. Phys. Chem.* **1992**, *96*, 1836.
(11) Lin, J.-L.; Bent, B. E. *J. Vac. Sci. Technol*. **1992**, *10* (4), 2202.
(12) Lin, J.-L.; Bent, B. E. *J. Phys Chem* **1993** , *97*, 9713.
(13) Chiang, C.-M.; Wentzlaff, T. H.; Jenks, C. J.; Bent, B. E *J. Vac. Sci. Technol*. **1992**, *10* (4), 2185.
(14) Kovacs, I.; Solymosi, F. *J. Phys Chem B* **1997**, *101*, 5397.
(15) Lamont C. L. A., Conrad H., Bradshaw A. M. *Surf. Sci.* **1993**, 280, 79.
(16) Roop, B.; Zhou, Y.; Liu, Z.-M.; Henderson, M. A.; Lloyd, K. G.; Campion, A.; White, J. M. *J. Vac. Sci. Technol*. A7 **1989** 2121.
(17) Lamont, C. L. A.; Conrad, H.; Bradshaw, A. M. *Surf. Sci.* **1993**, *287/288*, 169.
(18) Livneh, T.; Asscher, M. *J. Phys. Chem. B* **1997**, *101*, 7505.
(19) Livneh, T.; Asscher, M. *J. Phys. Chem. B* **1999**, *103*, 5665.
(20) Wolter, H.; Schmidt, M.; Wandelt, K. *Surf. Sci.* **1993**, *298*, 173.
(21) Kawaguchi, T.; Hijikigawa, M.; Hayafuji, Y.; Ikeda, M.; Fukushima, R.; Tomiie, Y. *Bull. Chem. Soc. Jpn.* **1973**, *46*, 53.
(22) Herzberg, G. *Molecular Spectra and Molecular Structure III: Electronic spectra and electronic structure of polyatomic molecules*; Van Nostrand Co. Inc.: Princeton, NJ, 1966; p 609.
(23) Chiang, C.-M; Bent, B. E *Surf. Sci.* **1992**, *279*, 79.
(24) Bange, K.; Dohl, R.; Grinder, D. E.; Sass, J. K. *Vacuum* **1983**, *33* (10−12), 757.
(25) Nagesha, K.; Fabrikant, I.; Sanche, L. *J. Chem. Phys.* **2001**, *114* (11), 4934.
(26) Tsekouras, A. A.; Iedema, M. J.; Cowin, J. P. *J. Chem. Phys.* **1999**, *111* (5), 2222.
(27) We note that our interpretation of a monolayer is different from other studies [refs 2−4 and 7] for which the definition of 1 ML is correlated with a definition of a bilayer (2 ML) in the present study.[18,19]
(28) Ellison, G. B.; Engelking, P. C.; Lineberger, W. C. *J. Am. Chem. Soc.* **1978**, *100* (8), 2556.